M. SZKLARSKA*,#, G. DERCZ*, J. RAK*, W. SIMKA**, B. ŁOSIEWICZ*

THE INFLUENCE OF PASSIVATION TYPE ON CORROSION RESISTANCE OF Ti15Mo ALLOY IN SIMULATED BODY FLUIDS

WPŁYW RODZAJU PASYWACJI POWIERZCHNI STOPU Ti15Mo NA JEGO ODPORNOŚĆ KOROZYJNĄ W ŚRODOWISKU PŁYNÓW USTROJOWYCH

This work reports on determination of the influence of passivation type of Ti15wt.%Mo implant alloy surface on its corrosion resistance in simulated body fluids. The alloy under investigation was subjected to natural self-passivation in air, and forced passivation by autoclaving in steam, boiling in 30 % solution of H_2O_2, and electrochemical passivation in 0.9 % NaCl solution. Resistance of the passivated Ti15Mo alloy to pitting corrosion was studied at 37ºC in 0.9 % NaCl solution using open circuit potential method, anodic polarization curves, and electrochemical impedance spectroscopy (EIS). Comparative estimation of the determined parameters of corrosion resistance revealed that the obtained passive layers improve anticorrosive properties of the tested alloy. Surface of the alloy subjected to passivation in steam autoclave reveals the highest protection against pitting corrosion. Anodic potentiodynamic curves showed that the Ti15Mo alloy after different passivation types of the surface is characterized by a lack of susceptibility to pitting corrosion up to potential of 9 V. Based on the EIS investigations, the thickness of the formed oxide layers (TiO_2, anatase) was determined to be in the range from 2.0 to 7.8 nm in dependence on the applied type of passivation. It was ascertained that electrochemical properties of the Ti15Mo alloy and possibility of its surface passivation using simple methods, make it an attractive material for use in biomedicine for long-term implants.

Keywords: biomaterial, electrochemical impedance spectroscopy, corrosion resistance, passivation, titanium alloys.

Praca dotyczy określenia wpływu rodzaju pasywacji powierzchni stopu Ti15%wag.Mo na jego odporność korozyjną w środowisku płynów ustrojowych. Badany stop poddano naturalnej samopasywacji w powietrzu oraz wymuszonej pasywacji w autoklawie parowym, w gotującym się 30 % roztworze H_2O_2 oraz elektrochemicznej pasywacji w 0,9 % roztworze NaCl. Odporność pasywowanego stopu Ti15Mo na korozję wżerową badano w temperaturze 37°C w roztworze 0,9 % NaCl metodą potencjału obwodu otwartego, krzywych polaryzacji anodowej oraz elektrochemicznej spektroskopii impedancyjnej (ESI). Ocena porównawcza wyznaczonych parametrów odporności korozyjnej wykazała, że wytworzone warstwy pasywne poprawiają właściwości antykorozyjne badanego stopu. Powierzchnia stopu poddana pasywacji w autoklawie parowym wykazuje najwyższą ochronę przed korozją wżerową. Anodowe krzywe potencjodynamiczne ujawniły, że stop Ti15Mo poddany różnym sposobom pasywacji powierzchni wykazuje brak podatności na korozję wżerową aż do potencjału wynoszącego 9 V. W oparciu o badania ESI wyznaczona została grubość otrzymanych warstw tlenkowych (TiO_2, anataz), która w zależności od zastosowanego sposobu pasywacji mieściła się w zakresie od 2,0 do 7,8 nm. Stwierdzono, że właściwości elektrochemiczne stopu Ti15Mo oraz możliwość pasywowania jego powierzchni prostymi metodami, czynią go atrakcyjnym materiałem do zastosowań w biomedycynie na implanty długoterminowe.

1. Introduction

Corrosion affects the fatigue strength leading to a mechanical failure of the implant working in the environment of body fluids [1]. In addition, corrosion products penetrating into the surrounding tissue can be toxic and cause infection and necrosis [2]. Therefore, one of the main indicators characterizing the biocompatibility of the biomaterial is its resistance to corrosion. With the increase in the corrosion resistance of biomaterial its biocompatibility is increasing. Implants made of metal with high corrosion resistance are covered with a protective oxide layer with a thickness of the order of magnitude of nanometers. A key factor in increasing the stability of such layers is their ability to self-repair. Furthermore, oxides formed on the implant surface should be poorly soluble in the tissue and should possess high thermodynamic stability [3], and also should protect against the harmful effects of metal, mainly aggressive chloride ions [4]. From this view-point, the passivation seems to be an attractive way to modify the surface of biomaterial that allows to limit the release of toxic metal ions during the implant contact with body fluids.

* UNIVERSITY OF SILESIA, INSTITUTE OF MATERIALS SCIENCE, SILESIAN INTERDISCIPLINARY CENTRE FOR EDUCATION AND RESEARCH, 75 PUŁKU PIECHOTY 1A, 41-500 CHORZÓW, POLAND
** SILESIAN UNIVERSITY OF TECHNOLOGY, FACULTY OF CHEMISTRY ,6 B. KRZYWOUSTEGO STR., 44-100 GLIWICE, POLAND
# Corresponding author: mszklarska@us.edu.pl

Titanium and its alloys due to their excellent mechanical properties, corrosion and biological inertness are one of the most popular materials used in implantology. Moreover, because of the high oxygen affinity these materials overlap stable, strongly adherent to the surface oxide layer which protects them against harmful environmental factors, e.g. human body [5]. Oxide layer is formed spontaneously - as a result of self-passivation, or by forced passivation which is carried out in certain conditions [6]. Addition of 15 wt.% of molybdenum to titanium is an optimal amount to reach the highest corrosion resistance and to slow pitting corrosion [7]. Moreover, Mo is well-known as an antioxidant, and element which is able to prevent cancer and anemia.

The following work concerned the corrosion properties of passive oxide layers on the Ti15Mo alloy received as a result of: (*i*) natural self-passivation, (*ii*) passivation using a steam autoclave, (*iii*) boiling in H_2O_2, and (*iv*) electrochemical passivation in simulated body fluid. Electrochemical corrosion resistance studies were carried out *in vitro* in 0.9% NaCl solution at 37°C. To determine the corrosion behaviour of the passive layers received on the Ti15Mo alloy the electrochemical studies by means of the open-circuit potential measurements, the method of anodic polarization curves, and the complementary technique of electrochemical impedance spectroscopy (ESI), were used.

2. Materials and experimental procedure

2.1. Material under investigation

Disk-shaped samples of the Ti15%wt.Mo alloy with a diameter of 10 mm were ground with 80 to 5000# grit silicon carbide paper and then ultrasonically cleaned in ultrapure water (Milli-Q, 18.2 MW cm^2, <2 ppb total organic carbon). The samples prepared in this way were subjected to four types of passivation: (i) natural self-passivation in air, (ii) passivation in steam using a steam autoclave Cominex for 30 min at 2.1 bar at 134°C, (iii) in boiling 30 % solution of H_2O_2 for 2 h, and (iv) electrochemical passivation at 5 V for 1 h in 0.9 % NaCl solution. The samples before electrochemical passivation were electrochemically depassivated at a potential equal to -1.2 V vs. saturated calomel electrode (SCE) for 10 min in 0.9 % NaCl solution.

The structure of the obtained oxide layers was characterized by X-ray studies using an X'Pert Philips PW 3040/60 diffractometer operating at 30 mA and 40 kV which was equipped with a vertical goniometer and an Eulerian cradle. The wavelength of radiation (λCuKα) was 1.54178A°. The grazing incidence X-ray diffraction (GIXD) patterns were registered in the 2θ range from 10 to 80° with a 0.05° step for the incident 0.15° angle. The microstructure was investigated using a JEOL JSM-6480 scanning electron microscope (SEM).

2.2. Corrosion test

Corrosion resistance of the passive layers was investigated in the deaerated with argon (Ar, 99.999% purity) 0.9 % NaCl solution at pH = 7.4 ± 0.1 under thermostatic conditions at 37 ±

2°C. During the investigation, a three-electrode electrochemical cell was used. The sample with the passive layer on its surface was the working electrode, the counter electrode was a Pt mesh and the reference electrode was the saturated calomel electrode (SCE) with a Luggin capillary. Only one side of the sample with an area of 0.785 cm^2 was subjected to the corrosion test, the rest of the electrode surface was covered with non-conductive and inert to the electrolyte epoxy resin. The measurements were carried out using a Metrohm/Eco Chemie Autloab PGSTAT30 Potentiostat/Galvanostat Electrochemical System.

Electrochemical studies began by measuring the open circuit potential (E_{OC}) until a stable potential value was occurred. Subsequently, the potentiodynamic studies were conducted in the potential range of ± 50 mV relative to the stabilized value of E_{OC} at a sweep rate v = 1 mV s^{-1}. Based on the registered polarization curves j = f (E), presented in the semi-logarithmic form, the Tafel extrapolation method was applied to determine the corrosion resistance parameters. The obtained results were the basis for comparison of corrosion resistance of the passive layers formed on the Ti15Mo alloy.

The EIS measurements were performed in the frequency range of 50 kHz - 1 mHz at a value of corrosion potential (E_{cor}) determined by the Tafel extrapolation method. Ten frequencies per decade were scanned using a sine-wave amplitude of 10 mV. *Ac* impedance data were analysed based on the concept of equivalent electrical circuits with respect to the physical meaning of the used circuit elements using the EQUIVCRT program.

Based on the following equation proposed by Birch and Burleigh [8] and experimental data obtained by EIS, the thickness of the formed oxide layers (d) was estimated:

$$d = \varepsilon_0 \varepsilon 2\pi S f (Z - Z_0) \qquad (1)$$

where: f – the frequency at which the phase angle (ϕ) reaches a maximum, Z – impedance at the frequency f, Z_0 – impedance at high frequencies (electrolyte resistance), S – area of the tested surface, ε_0 – dielectric for free space (8,854·10^{-12} F/m), ε – dielectric constant for TiO_2 (110).

Anodic polarization curves were registered potentiodynamically not later than 5 min after finishing the open circuit potential measurement at a sweep rate v = 5 mV s^{-1} in the potential range from Eoc minus 150 mV to 9 V.

3. Results and discussion

X-ray analysis confirmed the formation of an oxide layer on the Ti15Mo alloy surface modified by boiling in 30 % hydrogen peroxide solution (Fig. 1). Phase analysis revealed the presence of the following phases: α–Ti (ICDD PDF 03-065-3362), and β–Ti (ICDD PDF 01-089-4913). The broad reflection peaks at angles corresponding to the TiO_2 (anatase - ICDD PDF 01-071-1167) indicate the dispersion of crystallites formed in the passive layer. The oxide layers obtained by other passivation methods were too thin to be able to evaluate their structure by GIXD.
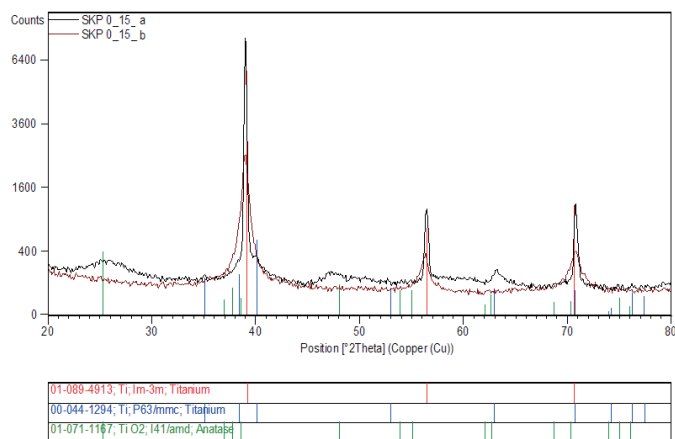
Fig. 1. XRD pattern of the Ti15Mo alloy undergoing: a) natural self-passivation, and b) boiled in 30 % H_2O_2

Corrosion resistance of the Ti15Mo alloy is dependent on the structure and thickness of the passive layer. As a result of contact the Ti15Mo alloy with the air, immediately and spontaneously on its surface a thin layer of oxide is formed in accordance with the following reactions:

$$Ti + O_2 \rightarrow TiO_2 \qquad (2)$$

Molybdenum does not react with air or oxygen at room temperature. At elevated temperatures the trioxide molybdenum(VI) oxide, MoO_3, is formed.

Corrosion resistance parameters of the Ti15Mo alloy subjected to different methods of surface modification were determined by the Tafel extrapolation method. Assuming a dissolution uniformity of each component of the Ti15Mo alloy and simultaneously excluding selective dissolution of Mo and Ti, the value of corrosion rate, CR, at E_{cor} was calculated based on the electrochemical measurements (Tafel characteristics) using the following equation according to the standard ASTM G 102-89 [9]:

$$CR = K_1 \frac{j_{cor}}{\rho} EW \qquad (3)$$

where: K_1 – calculation constant, j_{cor} – corrosion current density determined by the Tafel extrapolation. Density of the Ti15Mo alloy was estimated to be ρ = 4.96 g/cm³ [10]. Equivalent weight which is a dimensionless parameter was defined by the formula:

$$EW = \frac{1}{\sum \frac{n_i f_i}{M}} \qquad (4)$$

where: n_i – the valence of the i-th component of the alloy, f_i – the content of the i-th component in the metal, M_i – atomic mass of the i-th component of the alloy. Based on the Pourbaix diagram for Ti-H_2O and Mo-H_2O system [11], for the equilibrium potentials of the tested electrodes in 0.9 % NaCl solution (pH = 7.4), it was found that taken into account metals are present in thermodynamically stable form of Ti^{4+} and Mo^{6+}. The calculated EW value for the Ti15Mo alloy equalled 12.5.

The results of the Tafel extrapolation are summarized in Table 1. One can observe that the values of corrosion potential

of the modified alloy depend on the type of passivation and they were in the range from -0.181 to -0.038 V. The value of E_{cor} shifted towards noble potentials indicates the increase in corrosion resistance of the tested material. The determined values of corrosion current density and corrosion rate are characteristic for materials with very high corrosion resistance.

The indicative parameters show the highest corrosion resistance obtained for the Ti15Mo alloy passivated in an autoclave. The corrosion rate of the oxide layer formed in steam autoclave is only 3.545·10⁻⁴ mm/yr, while for the other passive layers it was higher one order of magnitude, 10⁻³ mm/yr. According to the literature data, CR of 0.001 mm/yr indicates the total resistance to pitting corrosion of tested material. The largest value of polarisation resistance and hence the highest corrosion resistance was determined for the sample boiled in 30 % H_2O_2 (R_p = 1.34·10⁵ Ω cm²), and next subjected to passivation in steam autoclave (R_p = 4.57·10⁴ Ω cm²).

The values of anodic, b_a, and cathodic, b_c, coefficient indicate that for all obtained oxide layers, anodic processes are faster than the cathodic ones. It is supposed that the corrosion process of the tested oxide layers will proceed via anodic dissolution.

Cathodic process taking place in an environment of 0.9 % NaCl can be the reduction of hydrogen ions according to the equation:

$$H^+ + e \rightarrow \frac{1}{2} H_2 \qquad (5)$$
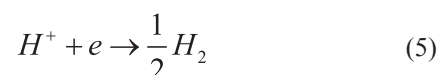
It can be expected that the occurring anodic process is the process of dissolution of the alloy component. As oxidation of titanium runs at high speed, it can not be the rate-limiting reaction of the anodic process. Therefore, it can be concluded that in accordance with thermodynamic data of Pourbaix diagram for the Mo-H_2O system [11], under applied electrochemical conditions the dissolution of molybdenum process is occurring:

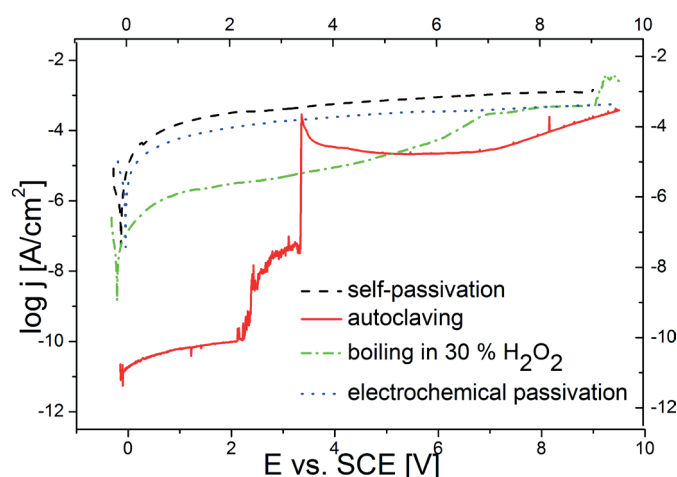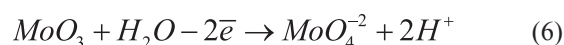$$MoO_3 + H_2O - 2\bar{e} \rightarrow MoO_4^{-2} + 2H^+ \qquad (6)$$

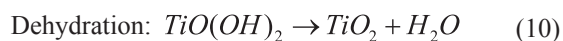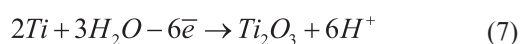Fig. 2. Anodic polarization curves (v = 5 mV / s) recorded in 0.9% NaCl solution for the passivated Ti15Mo alloy

2690

Summary of the corrosion resistance parameters determined by the Tafel extrapolation method for the passivated Ti15Mo alloy in 0.9 % NaCl solution
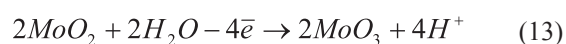
Passivation method*	1	2	3	4
E_{cor} [V]	-0.042±0.008	-0.164±0.033	-0.182±0.036	-0.051± 0.010
j_{cor} [A/cm^2]	$1.23±0.25·10^{-6}$	$4.07±0.81·10^{-8}$	$2.26±0.45·10^{-7}$	$1.04±0.21·10^{-6}$
b_c [V/dec]	0.063± 0.013	0.047±0.009	0.040±0.008	0.07±0.028
b_a [V/dec]	0.083±0.016	0.071±0.014	0.05±0.01	0.090±0.018
R_p [Ω cm^2]	$2.32±0.45·10^{3}$	$4.57±0.91·10^{4}$	$1.34±0.27·10^{5}$	$3.50±0.70·10^{3}$
CR at E_{cor} [mm/yr]	$1.01±0.20·10^{-2}$	$3.35±0.67·10^{-4}$	$1.86±0.37·10$-3	$8.57±1.71·10^{-3}$

*1 – self-passivation, 2 – autoclaving, 3 – boiling in 30 % H_2O_2, 4 – electrochemical passivation in 0.9 % NaCl

On the presented potentiodynamic characteristics (Fig. 2) there is no typical area of the active dissolution of the alloy due to the high content of titanium, which has the ability to passivation in air atmosphere according to Eq. 2, and thus the corrosion potential of the alloy is in the passive area of the anodic polarization curve. In the cases shown in Figure 2 it is seen that in the range of potentials from E_{cor} up to 9 V the tested alloy is located in the passive area. In the range of potentials lower than 0.1 V occurs a formation of titanium oxides of a lower oxidation states (TiOOH, Ti_2O_3), above this potential the Ti^{3+} is oxidise to Ti^{4+}. The oxides are formed according to reactions [12,13]:

$$2Ti + 3H_2O - 6\overline{e} \rightarrow Ti_2O_3 + 6H^+ \qquad (7)$$

$$Ti_2O_3 + 3H_2O - 2\overline{e} \rightarrow 2TiO(OH)_2 + 2H^+ \qquad (8)$$

$$Ti + 3H_2O - 4\overline{e} \rightarrow TiO(OH)_2 + 4H^+ \qquad (9)$$

$$\text{Dehydration: } TiO(OH)_2 \rightarrow TiO_2 + H_2O \qquad (10)$$

The anodic polarization of molybdenum leads to the formation of MoO and MoO_2 oxides at the potential range from -0.20 to 0.20 V. These oxides partially oxidise to MoO_3 at potential higher than 0.40 V [14] according to the following reactions:

$$Mo + H_2O - 2\overline{e} \rightarrow MoO + 2H^+ \qquad (11)$$

$$MoO + H_2O - 2\overline{e} \rightarrow MoO_2 + 2H^+ \qquad (12)$$

$$2MoO_2 + 2H_2O - 4\overline{e} \rightarrow 2MoO_3 + 4H^+ \qquad (13)$$

With increasing the potential value the stabile oxide layer growth thicker. The oxide layer is mainly composed with TiO_2, hydrated TiO_2 and Ti_2O_3, and small amount of MoO_3 what is

caused by faster migration of Ti^{4+} ions to the surface than Mo^{6+} ions [13,15,16].

Based on the potentiodynamic characteristics in a wide range of potentials (Fig. 2) it can be concluded that the Ti15Mo alloy subjected to self-passivation and electrochemical passivation shows very similar electrochemical properties in physiological saline. No initiation of pitting corrosion up to the potential of 9 V was observed (Fig. 2). The polarization curve log j = f(E) obtained for the alloy passivated by autoclaving shows the resistance of the passive layer to anodic dissolution up to the potential of 2.25 V. With further potential growth a significant increase in current density is observed which can indicate the break-down of protection layer at a potential equal to 3.37 V. For more anodic potential values of creation and dissolution of the oxide layer occur simultaneously. In the range of potentials from 5.16 to 7.25 V a broad plateau which evidence the protective properties of the formed oxide layer occurs and it can be related to transpassivation process. The oxide layer still protects the substrate against pitting corrosion but at higher current density values as it was observed before its break-down at E = 2.25 V. Anodic dissolution of the transpassive layer begins above 7.25 V. Whereas for the samples modified by boiling in hydrogen peroxide dissolution of the oxide layer begins at a potential equal to 9 V. It should be added that a typical initiation of pitting potentials observed for titanium and its common alloys in SBF environment stands at around 2 V vs. SCE [17]. Current densities for the autoclaving sample are 5 orders of magnitude lower than for the tested alloy passivated by other methods. Those results indicate that the slowest corrosion processes occur for the oxide layer formed in steam.

The experimental data obtained by EIS were shown graphically in Bode diagrams (Figs. 3 and 4). The Bode plots in the frequency range between 50 kHz and 1 mHz present only one time constant and a near-capacitive response with a phase angle close to 80° and linear variation between log |Z| and log f, at a wide range of frequencies, with a slope close to -1.

Comparative corrosion resistance evaluation of the passive layers was performed according to the log | Z | at f = 1 mHz. The highest corrosion resistance exhibits alloy passivated using a steam autoclave (log | Z |$_{f = 1\,mHz}$ = 5.98 Ω cm^2) and boiled in 30% H_2O_2 (log | Z |$_{f = 1\,mHz}$ = 5.18 Ω cm^2). In case of other passivation methods of the Ti15Mo alloy there was observed a decrease in the value of log | Z |$_{f = 1\,mHz}$ to about 4-4.5 Ω cm^2.

Bode diagram showing an experimentally determined relationship of phase angle as a function of frequency φ = f

(logf) shown in Fig. 4 is a typical impedance spectrum for the oxide layer on a titanium substrate, with a characteristic broad plateau at intermediate frequencies. One time constant in the circuit suggests that the corrosion process proceeds by one step via anodic dissolution.
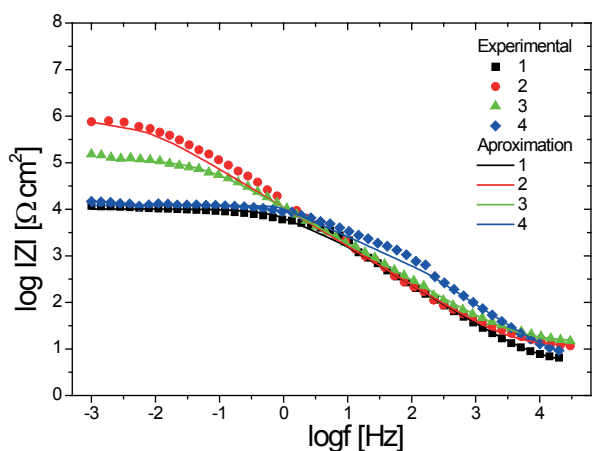

Fig. 3. Experimental (symbol) and approximated (line) Bode diagrams in the form of log | Z | = f (log f) in 0.9 % NaCl solution for the passivated Ti15Mo alloy. 1 – self-passivation, 2 – autoclaving, 3 – boiling in 30 % H_2O_2, 4 – electrochemical passivation in 0.9 % NaCl
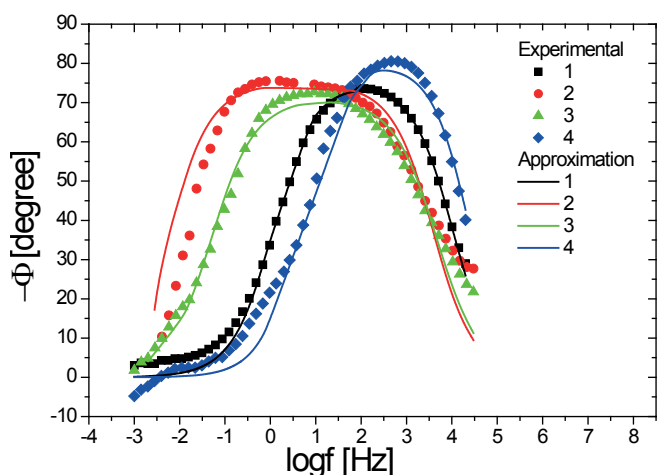

Fig. 4. Experimental and approximated (line) Bode diagrams in the form of j = f (log f) in 0.9 % NaCl solution for the passivated Ti15Mo alloy. 1 – self-passivation, 2 – autoclaving, 3 – boiling in 30 % H_2O_2, 4 – electrochemical passivation in 0.9 % NaCl

The experimental impedance spectra were approximated using an equivalent electrical circuit (EEC) of Randle's cell representing the physical model of the oxide layer | SBF system (Fig. 5). In this model, R_s represents resistance of the solution, R_{ox} is the resistance of charge transfer through the oxide layer | SBF interface, and the electrical double layer capacitance parameter, C_{dl}, corresponds to ideal capacitor. To approximation procedure instead of a capacitor the constant phase element (CPE) was used [18]. Its impedance is:

$$\hat{Z}_{CPE} = \frac{1}{T(j\omega)^\phi} \tag{14}$$

where T (in F cm^{-2} s$^{\phi-1}$) denotes the capacitance parameter and $\phi \leq 1$ is a dimensionless CPE exponent related to the constant phase angle, $\alpha = 90°(1-\phi)$.
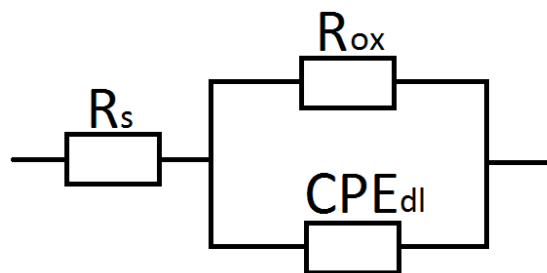

Fig. 5. Randle's equivalent circuit model used to analyze metallic biomaterial surface electrochemical impedance properties

Results of approximation were summarized in Table 2 and presented on Bode plots in the form of continuous line (Figs. 3 and 4). All impedance spectra could be well approximated by the equivalent electrical circuit in Fig. 5 which is typically used to describe oxide thin film surfaces. The error of the particular parameter determination was always below 20 %. The value of ϕ_{dl} parameter is associated with surface roughness and for the most porous oxide layer obtained by boiling in H_2O_2 its value was 0.79. The R_{ox} parameter was characterized by the highest value for the samples after autoclaving (7.60·10^5 Ω cm^2) and points the strongest protective properties of the formed oxide layers. The R_{ox} values are in a very good agreement with the polarization resistance data obtained by anodic polarization measurements (Table 1).

The C_{dl} values for the formed oxide layer | SBF system were determined from the Brug formula [19]:

$$T = C_{dl}^\phi(R_s^{-1} + R_{ct}^{-1})^{1-\phi} \tag{15}$$

Based on data obtained by electrochemical impedance spectroscopy and the model proposed by Birch and Burleigh'a [8], the thickness of the passive layers was estimated. The results were summarized in Table 3. The thickness of the

TABLE 2

Summary of the parameters obtained using the Randle's equivalent circuit model shown in Fig. X to approximate EIS data for the passivated Ti15Mo alloy in 0.9 % NaCl solution at 37°C.

Passivation method	R_s [Ω cm^2]	R_{ox} [Ω cm^2]	T_{dl} [F cm^{-2} s$^{\phi-1}$]	ϕf_{dl}	C_{dl} [F cm^{-2}]
self-passivation	4.83	1.01·10^4	2.35·10^{-6}	0.838	2.58·10^{-7}
autoclaving	11.39	7.60·10^5	2.24·10^{-6}	0.833	2.67·10^{-7}
boiling in 30 % H_2O_2	14.13	1.19·10^5	1.23·10^{-6}	0.792	6.91·10^{-8}
electrochemical passivation in 0.9 % NaCl	5.56	1.21·10^4	1.05·10^{-6}	0.896	2.59·10^{-7}

oxide layers, depending on the passivation method were in the range from 2.0 to 7.8 nm.

TABLE 3

The thickness of the oxide layer formed on the Ti15Mo alloy by different passivation methods.

Passivation method of Ti15Mo alloy	d [nm]
self-passivation	2.0±0.4
autoclaving	2.8±0.6
boiling in 30 % H_2O_2	7.8±1.6
electrochemical passivation in 0.9 % NaCl	3.8±0.8

Morphology of the obtained oxide layers on the Ti15Mo surface before and after corrosion tests were observed using SEM. Microscopic analysis showed a strong influence of the type of passivation on the surface morphology (Fig. 6). The alloy passivated in boiling 30 % H_2O_2 is characterized by the most developed surface morphology. Microphotographs also revealed that the surface obtained by electrochemical passivation was smoother in comparison to starting sample mechanically polished. On the samples surface tested by potentiodynamic methods with anodic potential limited to 9 V, there was no pitting characteristic to electrochemical corrosion of metallic implants in an environment containing aggressive anions, Cl$^-$. Addition of molybdenum stabilized the passive films against breakdown and pit initiation could be slowed down or primary suppressed in comparison with pure Ti [20].

The initially porous surface of the sample passivated in boiling 30 % H_2O_2 was a slightly smoother after corrosion tests (Fig. 6f), what was correlated with the anodic polarization curves, where the slow dissolution of the passive layer was observed. The potential value of 9.5 V was found as a beginning of micro-pits formation on the oxide layer formed in boiling hydrogen peroxide.
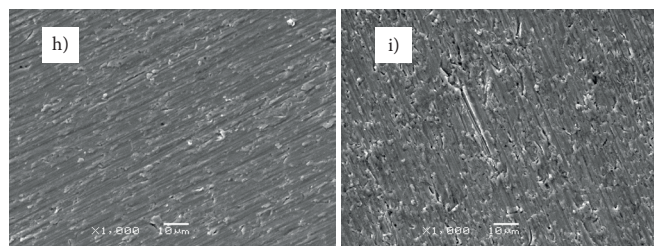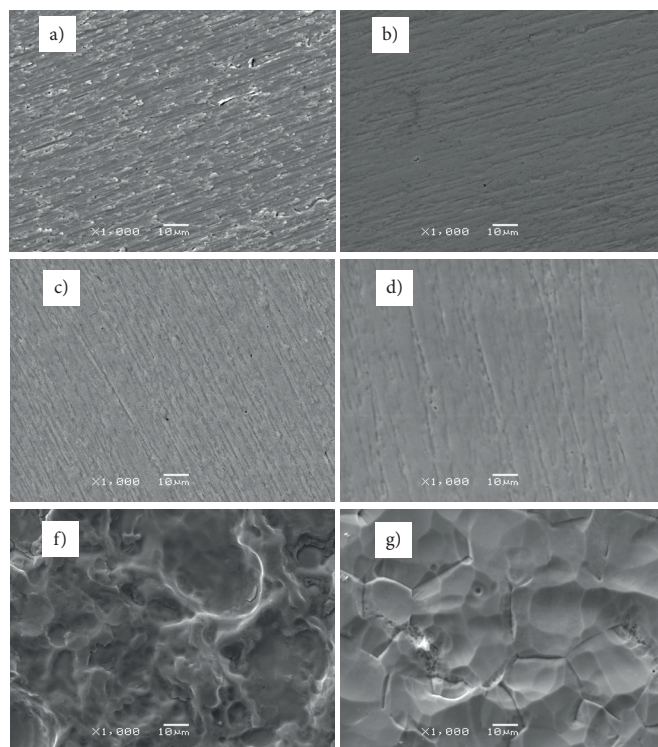

Fig. 6. Morphology Ti15Mo alloy passivated by different methods before and after corrosion tests: a, b – self-passivation in the air, c, d – electrochemical passivation at 5 V for 1 h w 0.9 % NaCl solution, e, f – boiling in 30 % H_2O_2 for 2 h, g, h – passivation in steam autoclave for 30 min, at a pressure of 2.1 bar and at 134°C

4. Conclusion

The conducted study shows that the Ti15Mo alloy has a high corrosion resistance in environment of SBF. Based on the results of corrosion tests obtained by conventional electrochemical methods coupled with a complementary method of electrochemical impedance spectroscopy it can be concluded that additional surface modifications by the different passivation types, improves the corrosion properties of the Ti15Mo alloy. There was observed no pitting corrosion up to potential of 9 V for all tested samples. The values of corrosion current density for the alloy subjected to forced passivations are lower in comparison to the sample with the layer formed as a result of natural self-passivation. The increase in the polarization resistance values proves that the used surface passivation methods contributed to the increase the corrosion resistance of the Ti15Mo alloy by forming the barrier layers of TiO_2 (anatase) with a thickness of 2.0 to 7.8 nm.

As a result of electrochemical passivation in 0.9% NaCl solution a small improvement of corrosion properties was achieved. The best corrosion resistance, result from passivation in a steam autoclave and boiling 30 % H_2O_2. The values of log $| Z |_{f = 1 \, mHz}$ for such passivated alloy are around 6 - 5 Ω cm^2. The corrosion rate for these samples is in the range of 10^{-4} - 10^{-3} mm/yr. As a result of passivation in steam autoclave the smooth surface was achieved, whereas passivation in boiling 30 % hydrogen peroxide gave porous/rough passive layer. The more developed implant surface may favour the incorporation of the bioactive nanoparticles or drugs.

REFERENCES

[1] M. Geetha, U. Kamachi Mudali, A.K. Gogia, R. Asokamani, R. Baldev, Corros. Sci. **46,** 877-892 (2004).

[2]   M. Freitag, B. Łosiewicz, T. Goryczka, J. Lelątko, Solid State Phenom. **183,** 57-64 (2012).

[3] J. Szewczenko, J. Marciniak, M. Kaczmarek, Eng. Biomat.

106-108, 21-25 (2011).

[4] T. Błaszczyk, B. Burnat, L. Klimek, H. Scholl, Eng. Biomat. **96-98,** 10-15 (2010).

[5] M. Papakyracou, H. Mayer, C. Pypen, H. Plenk Jr, S. Stanzl-Tschegg, Int. J. Fatigue **22,** 873-886 (2000).

[6] S. Shabalovskaya, J. Anderegg, J. Van Humbeeck, Acta Biomater. **4,** 447-467 (2008).

[7] N.T.C. Oliviera, A.C. Guastaldi, Acta Biomater. **5,** 399-405 (2009).

[8] J.R. Birch, T.D. Burleigh, Corrosion, **56,** 1233-1241 (2000).

[9] ASTM G 102-89: „Standard Practice for Calculation of Corrosion Rates and Related Information from Electrochemical Measurements".

[10] J. Disegi, Implant Materials Wrought-15% Molybdenum, Synthes, West Chester 2009.

[11] N. Takeno, Atlas of Eh-pH diagrams. Intercomparision of thermodynamic databases. Open File Report No. 419. National Institute of Advanced Industrial Science and Technology, Geological Survey of Japan, Tokyo, Japan 2005.

[12] M. Metikos-Hukovic, A. Kwokal, J. Piljac, Biomaterials **24,** 3765-3775 (2003).

[13] W. Simka, Electrochim. Acta, **56,** 9831-9837 (2011).

[14] K. Wang, Y.S. Li, P. He, Electrochim. Acta, **43,** 2459-2467 (1998).

[15] Y.L. Zhoua,, D.M. Luob, J. Alloys Compd. **509,** 6267–6272 (2011).

[16] H. Habazakia, M. Uozumia, H. Konnoa, S. Nagatab, K. Shimizuc, Surf. Coat. Technol. **169 –170,** 151–154 (2003).

[17] Z. Lekston, B. Łosiewicz, A. Winiarski, M. Jędrusik-Pawłowska, M. Kromka-Szydek, K. Miernik, Eng. Biomat. **96-98,** 29-33 (2010).

[18] A. Lasia, in: B.E. Conway, J.O'M. Bockris, R.E. White (Eds.), Modern Aspects of Electrochemistry **35,** Kluwer/Plenum, New York (2002).

[19] H. Morawiec, J. Lelątko, A. Winiarski, G. Stergioudis, T. Goryczka, P. Pączkowski, Eng. Biomat. **37,** 32 (2004).

[20] A. Pardo, M.C. Merino, A.E. Coy, F. Viejo, R. Arrabal, E. Matykina, Corros. Sci. **50,** 1796-1806 (2008).